Design Considerations for Iteratively-Decoded Source-Channel Coding Schemes

Ragnar Thobaben* and Jörg Kliewer†

*University of Kiel, Institute for Circuits and Systems Theory, 24143 Kiel, Germany
†Department of Electrical Engineering, University of Notre Dame, Notre Dame, IN 46556, U.S.A.

***Abstract*— We address outer variable-length encoding of a first-order Markov source in a serially concatenated coding scheme with an inner recursive convolutional code. Decoding is carried out iteratively between the constituent decoders for variable-length and convolutional code. While variable-length codes are commonly known to be sensitive to transmission errors, we show that they can lead to significant performance improvements compared to fixed-length source encoding with optimized mappings. Specifically, we propose a simple variable-length code construction with a free distance of two and good compression properties at the same time. Numerical results show that the performance gain of the proposed approach also holds for precoded ISI channels where iterative joint source channel equalization and decoding is employed at the receiver.**

I. Introduction

The robust transmission of variable-length encoded source signals over wireless channels has become an active research area during the last years. It is motivated by the increasing demand on multimedia and data services in third and fourth generation wireless networks. In such applications source compression is usually carried out using standardized techniques which, in order to achieve high compression gains, often employ variable-length codes (VLCs).

VLCs were originally designed for error-free transmission scenarios. In this form they are highly sensitive to transmission errors and suffer from error propagation; for example, single bit errors may lead to insertions and deletions of symbols, causing a loss of synchronization. For this reason, VLCs are usually avoided in classical wireless communication applications.

In order to make VLCs applicable to the peculiarities of wireless channels, a variety of joint source-channel coding and decoding schemes addressing the error-resilient transmission of VLCs have been proposed in the literature. This includes the design of error-resilient VLCs, the joint optimization of VLCs and channel codes, the robust decoding of VLCs, and the joint decoding of VLCs and channel codes. For delay- and / or complexity-constrained transmission scenarios those combined techniques are often more advantageous than the classical separation of source and channel encoding. As we will show in the following, such schemes have the potential to even outperform schemes based on fixed word length source encoding, which are usually not affected by synchronization problems.

A class of robust VLCs is given by reversible variable-length codes (RVLCs) [1–4], which are a well established technique for robust video compression. RVLCs exploit additional redundancy in the VLC code words in order to guarantee bidirectional decoding. If the number of error events is low, the impact of a synchronization loss can be mitigated. In [5], Buttigieg introduced variable-length error-correcting codes (VLECs), which combine the variable-length character of VLCs with distance constraints of channel codes at the cost of additional redundancy.

A key component for a reliable transmission of VLCs is given by the VLC decoder. The first maximum *a posteriori* probability (MAP) decoder was introduced in [6], where an optimal VLC sequence estimation was carried out by the Viterbi algorithm, applied to an appropriate VLC trellis. Another trellis representation, which has become the standard trellis for VLC decoding, was introduced in [7]. It benefits from an efficient state representation and allows both a bitwise MAP and *a posteriori* probability (APP) decoding with the BCJR algorithm [8] and an optimal sequence estimation with the Viterbi algorithm. Later on, both exact and complexity-reduced approximate MAP decoding techniques for variable-length source codes were proposed by different authors, either by using a modified or list Viterbi algorithm [9–14] or by using sequential decoding approaches [15], [16].

Many approaches (e.g., [10–12]) exploit the redundancy due to the residual source correlation after source encoding for additional error protection. Generally, this allows for a less powerful forward error correction (FEC) code, resulting in a reduction of allocated bandwidth or latency for the overall transmission system. As reported in [17–21], a significant amount of residual source correlation, modeled as first-order Markov process, can be observed for several output parameters in state-of-the-art speech codecs and the MPEG audio compression scheme. For some parameters, even a redundancy up to 50% can be observed.

Further improvements can be achieved by additional forward error correction combined with a joint decoding of source and channel code. Depending on the encoder structure, this can be obtained by merging the source and the channel decoder, as proposed in [9], [22–24]. Since the concatenation of VLC and channel code essentially represents a serial code concatenation, another option is to apply iterative

This work was partly supported by the German Research Foundation (DFG) under grant KL 1080/3-1 and by the University of Notre Dame Faculty Research Program.

source-channel decoding (ISCD), which was proposed by Bauer and Hagenauer [25] for VLCs and by Goertz in [26] for fixed-length mappings. Further ISCD approaches for VLCs were presented by several authors [27–33] and differ in the realization of the employed soft-input / soft-output VLC decoder.

In the following, we address the joint design of source and channel encoding for ISCD. While earlier work in [34], [35] focuses on the trade-off between the explicit redundancy introduced by the channel and the source encoder, we consider correlated source signals and rate-1 channel codes. The resulting encoding schemes are optimized both in terms of convergence properties and error-floor performance based on the design guidelines for serial concatenated codes given in [36], [37] and an analysis of the extrinsic information transfer characteristics [38]. Specifically, we propose a novel variable-length code construction with a minimum Hamming distance of two which allows the resulting source-channel encoding and decoding scheme to outperform the best known fixed-length mappings for ISCD [39] *without* introducing additional redundancy. Simulation results are presented for a binary transmission over the AWGN channel, where we also address the case of additional inter-symbol interference (ISI).

This paper is organized as follows. Section II presents an overview of the transmission system and iterative source-channel decoding. In Section III we propose a novel VLC code construction which is specifically tailored to the system being optimized in Section IV. Finally, simulation results are given in Section V.

II. Transmission System

We consider the scenario depicted in Fig. 1, where the transmission of a source-channel encoded real-valued source $\mathbf{U}$[1] over a white Gaussian noise (AWGN) channel with additional ISI is addressed.

A. Source Model and Source Encoder

In the following, we address the case where redundancy due to both residual intraframe correlation and non-uniform source symbol distribution is inherent in the source signal. Therefore, we assume that the source vector $\mathbf{U}$ consists of K real-valued correlated source symbols $U_k \in \mathbb{R}$, which may be generated by a first-order autoregressive process. Such a source process can be obtained by filtering uncorrelated Gaussian noise with a recursive filter $H(z) = z/(z-a)$ where a is the correlation coefficient.

After W-bit quantization, we obtain the index vector $\mathbf{I}$ with elements $I_k \in \mathbb{I}$, $\mathbb{I} = \{0, \ldots, 2^W - 1\}$, drawn from the distribution $\Pr(I_k)$. The residual index correlation is modeled by a first-order Markov process, characterized by the index-transition probabilities $\Pr(I_k|I_{k-1})$. These probabilities are later exploited at the receiver side as additional *a priori* knowledge, leading to an enhanced error protection. In this context, they may be interpreted as a *soft parity check*.

[1]Random variables and vectors of random variables are represented by upper-case letters, the corresponding realizations are represented by lower-case letters.

In a final encoding step, the quantization indices I_k are mapped symbol-wise to their binary representation, resulting in a length-N bit vector with elements $B_n \in \{0, 1\}$. For comparison purposes we consider mappings realized by variable-length codes (VLCs) with the codeword set $\mathcal{VLC}$ and the mean word length $\bar{l}$ and also mappings with a fixed word length W.

B. Channel Encoder and Precoder

After source encoding, the binary source vector $\mathbf{B}$ is permuted by an interleaver π. The resulting bit vector $\mathbf{B}'$ with elements $B'_{n'}$ is the input to the channel encoder, which consists of a recursive systematic convolutional (RSC) code with rate $R_{RSC} = 1$, punctured from a rate-1/2 mother code with generator polynomials $(G_r, G_f)_8$. G_r denotes the feedback polynomial and G_f the feedforward polynomial.

In the absence of ISI, the RSC encoder serves as an inner scrambler. Puncturing is then performed randomly such that a fraction of $p_{sys} \in [0, 1]$ of the systematic bits and a fraction of $p_{par} = 1 - p_{sys}$ of the parity bits are removed from the bit stream. This puncturing method is beneficial since, for a given mother code, an optimization relies solely on the parameter p_{sys}. If an additional degradation by ISI is considered, the RSC encoder serves as a recursive rate-1 precoder. In this case, all systematic bits are punctured ($p_{sys} = 1$). Furthermore, we restrict ourselves to the case where the precoder solely consists of a feedback polynomial.

C. Channel Model

In the following, we consider a binary transmission employing binary phase shift keying (BPSK); i.e., the symbols X_m at the output of the encoder are taken from the set $\{-1, 1\}$. The ISI on the channel is modeled by a real-valued linear filter with the finite impulse response $h_0(m)$. If no ISI is considered, $h_0(m) = \gamma_0(m)$ holds with $\gamma_0(m) = 1$ for $m = 0$ and $\gamma_0(m) = 0$ for $m \neq 0$. We apply a normalization of the impulse response $h_0(m)$ such that $E_s = E\{|X|^2\} = E\{|Z|^2\} = E_z$. An additional white Gaussian noise process $\mathbf{N}$ with the noise variance $\sigma_N^2 = 1/(2E_s/N_0)$ is then added to the output $\mathbf{Z}$ of the ISI filter. Correspondingly, the observations Y_m at the output of the channel are characterized by the likelihood $p_{Y|Z}(y|z)$.

D. Iterative Source-Channel Decoder and Equalizer

The realized transmitter structure is equivalent to a serial concatenation of two component codes which are separated by an interleaver [36]. Accordingly, both joint decoding of the source and channel code and joint source decoding and equalization of the ISI channel can be realized by the iterative decoding scheme depicted in Fig. 1. In the following, we give a brief description of the iterative source-channel decoder discussed in [33], which is here extended to the case of transmission channels suffering from ISI. For further reading we refer to [33].

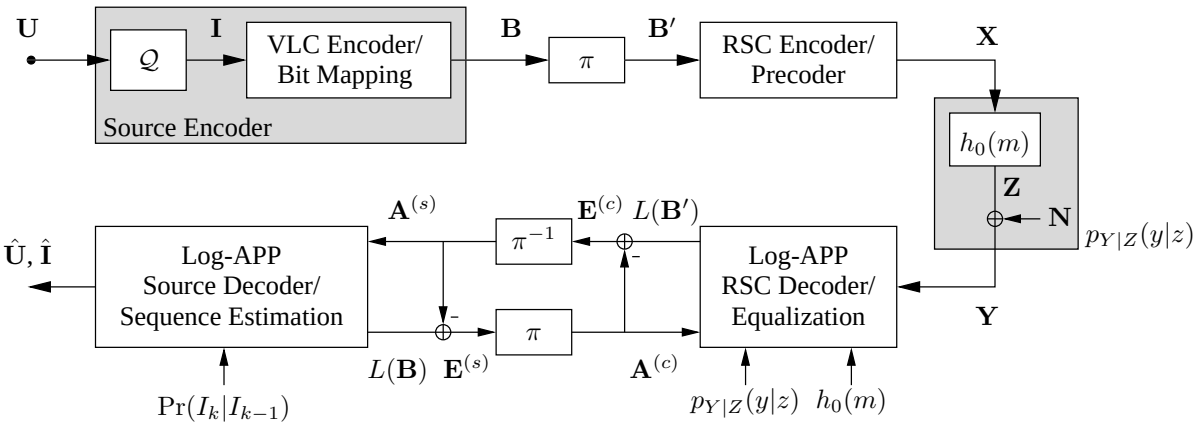

Fig. 1. Model of the transmission system, containing source encoding, channel encoding / precoding, and iterative source channel decoding for the AWGN channel, and iterative source decoding and equalization in the case of inter-symbol interference.

1) Component Decoders: The iterative decoder consist of two soft-input / soft-output (SISO) decoders, corresponding to the outer source encoder and the inner channel encoder / ISI channel. All decoders are realized by trellis-based *a posteriori* probability (APP) decoders. They are implemented in the logarithmic domain (Log-APP decoder) and provide log-likelihood ratios (LLRs) [40] for the corresponding symbols at the encoder side.

Based on the observations $\mathbf{Y} = [Y_1, \ldots, Y_M]$ for the transmitted symbols X_m at the output of the communication channel and on the *a priori* information $\mathbf{A}^{(c)} = [A_1^{(c)}, \ldots, A_N^{(c)}]$ for the interleaved symbols $B'_{n'}$, the inner decoder computes the vector

$$L(\mathbf{B}') := \Big[L(B'_1 \,|\, \mathbf{Y}, \mathbf{A}^{(c)}), \ldots, L(B'_N \,|\, \mathbf{Y}, \mathbf{A}^{(c)})\Big]$$

of *a posteriori* LLRs for the interleaved source bits $B'_{n'}$

$$L(B'_{n'} \,|\, \mathbf{Y}, \mathbf{A}^{(c)}) := \ln\left(\frac{\Pr(B'_{n'}=0 \,|\, \mathbf{Y}, \mathbf{A}^{(c)})}{\Pr(B'_{n'}=1 \,|\, \mathbf{Y}, \mathbf{A}^{(c)})}\right).$$

Hence, if no ISI is present on the channel, we apply the BCJR algorithm [8] to the trellis representation of the underlying RSC code. In the case of ISI, the RSC trellis is replaced by a super trellis for the ISI channel and the recursive precoder, which can be seen as a generalization of the DPSK/ISI super trellis proposed in [41]. In order to construct the super trellis, the precoder and the filter associated with the ISI are combined to a single encoder with a binary feedback polynomial and a real-valued feedforward polynomial similar to the direct form II realization for recursive real-valued filters [42]. Correspondingly, for binary input sequences the trellis states of the super trellis can be directly obtained from the states of this filter. We also assume that perfect knowledge of the noise statistics $p_{Y|Z}(y \,|\, z)$ and the channel impulse response $h_0(m)$ is available at the decoder.

For the outer source decoder we consider the Log-APP VLC decoder proposed in [33]. By appropriate modifications of the classical BCJR algorithm for the trellis proposed in [7] the residual source correlation can be exploited for additional error protection. Due to a low number of trellis states this results in an efficient decoding algorithm which is especially well-suited for the decoding of large block lengths.

Similar to the inner encoder, the outer decoder computes the vector

$$L(\mathbf{B}) := \Big[L(B_1 \,|\, \mathbf{A}^{(s)}), \ldots, L(B_N \,|\, \mathbf{A}^{(s)})\Big]$$

of *a posteriori* LLRs on the source bits B_n

$$L(B_n \,|\, \mathbf{A}^{(s)}) := \ln\left(\frac{\Pr(B_n=0 \,|\, \mathbf{A}^{(s)})}{\Pr(B_n=1 \,|\, \mathbf{A}^{(s)})}\right)$$

by considering additional *a priori* knowledge in form of the index-transition probabilities $\Pr(I_k|I_{k-1})$. Since the outer decoder decodes on the VLC codebits and not on the symbols of the desired source index vector $\mathbf{I}$, a subsequent sequence estimation on the VLC trellis [7] must be employed in order to obtain the index and source vector estimates $\hat{\mathbf{I}}$ and $\hat{\mathbf{U}}$.

2) Iterative Decoding: The iterative decoding process is based on the exchange of extrinsic information [40] between the two component decoders. Therefore, the *a posteriori* LLRs $L(B'_{n'} \,|\, \mathbf{A}^{(c)}, \mathbf{Y})$ and $L(B_n \,|\, \mathbf{A}^{(s)})$ of the two decoders are separated into two terms corresponding to the *a priori* information $A_{n'}^{(c)}$ and $A_n^{(s)}$ and the extrinsic information $E_{n'}^{(c)}$ and $E_n^{(s)}$. By employing the notation $\mathbf{X}_{\setminus n} = [X_1, \ldots, X_{n-1}, X_{n+1}, \ldots, X_N]$ and under the assumption of equiprobable bits $B'_{n'}$ and B_n we obtain[2]

$$L(B'_{n'} \,|\, \mathbf{A}^{(c)}, \mathbf{Y}) = \underbrace{L(B'_{n'} \,|\, \mathbf{A}^{(c)}_{\setminus n'}, \mathbf{Y})}_{=:E_{n'}^{(c)}} + \underbrace{L(B'_{n'} \,|\, A_{n'}^{(c)})}_{=A_{n'}^{(c)}} \quad (1)$$

for the inner channel decoder / equalizer and

$$L(B_n \,|\, \mathbf{A}^{(s)}) \;=\; \underbrace{L(B_n \,|\, \mathbf{A}^{(s)}_{\setminus n})}_{=:E_n^{(s)}} \;+\; \underbrace{L(B_n \,|\, A_n^{(s)})}_{=A_n^{(s)}} \quad (2)$$

for the outer source decoder.

The *a priori* LLRs $A_{n'}^{(c)}$ and $A_n^{(s)}$ are direct observations of the binary symbols $B'_{n'}$ and B_n, respectively, while the extrinsic LLRs $E_{n'}^{(c)}$ and $E_n^{(s)}$ carry the information

[2]Note that for the LLRs $A_n^{(\cdot)}$ the identity $L(B_n \,|\, A_n^{(\cdot)}) = A_n^{(\cdot)}$ holds.

provided by the remaining observations $\mathbf{A}_{\setminus n'}^{(c)}$, $\mathbf{Y}$, and $\mathbf{A}_{\setminus n}^{(s)}$, respectively. According to (1) and (2), with the notation

$$\mathbf{E}^{(s)} = [E_1^{(s)}, \ldots, E_N^{(s)}] \quad \text{and} \quad \mathbf{E}^{(c)} = [E_1^{(c)}, \ldots, E_N^{(c)}],$$

the extrinsic LLRs $E_{n'}^{(c)}$ and $E_n^{(s)}$ can be obtained by subtracting the *a priori* input $A_{n'}^{(c)}$ and $A_n^{(s)}$ from the *a posteriori* LLRs $L(B'_{n'} \,|\, \mathbf{A}^{(c)}, \mathbf{Y})$ and $L(B_n \,|\, \mathbf{A}^{(s)})$ as shown in Fig. 1. After (de-)interleaving, the extrinsic LLRs provided by the one decoder become the *a priori* input of the other decoder. Since no extrinsic information is available at the output of the outer decoder during the initial decoding step, the *a priori* LLRs $A_{n'}^{(c)}$ of the inner decoder are initialized with zeros.

The iterative process continues until an error-free transmission is achieved or an appropriate stopping criterion is satisfied. Note that after the first half iteration the quantities derived by the inner Log-APP decoder are no longer exact *a posteriori* LLRs: BJCR-based standard decoders consider the input vectors $\mathbf{Y}$ and $\mathbf{A}^{(c)}$ to be mutually independent. But in fact, the *a priori* input $\mathbf{A}^{(c)}$ is a function of $\mathbf{Y}$. Thus, exact *a posteriori* LLRs may only be obtained if the Log-APP decoder addresses these dependencies in the derivation of the LLRs.

E. Code Rate of the Transmission System

Since the source correlation ameliorates the achievable error protection, the overall code rate R of the transmission system relies on both the explicit redundancy of the channel code and the amount of residual source redundancy. Therefore, we associate the source redundancy with a code rate R_S. Due to the serial concatenation of source and channel encoding, the overall code rate R of the transmission system is then given by the product of the code rate R_S of the source encoder and the code rate R_{RSC} of the RSC code: $R = R_S \cdot R_{RSC}$.

With the entropy $H(\mathbf{B})$ of the vector $\mathbf{B}$, we can define the code rate R_S of the source signal as

$$R_S := \frac{H(\mathbf{B})}{N} = \frac{H(\mathbf{B})}{K \cdot \bar{l}},$$

where $\bar{l} = W$ for a fixed word length with W-bit quantization.

The code rate R_S can be separated into the product of two code rates R_{corr} and R_{Map}. While the code rate R_{corr} corresponds to the redundancy due to the intraframe correlation, the code rate R_{Map} is associated with the redundancy introduced by the bit mapping or the VLC. With $H(\mathbf{B}) = H(\mathbf{I})$ we obtain

$$R_S = \underbrace{\frac{H(\mathbf{I})}{K \cdot H(I_k)}}_{=:R_{corr}} \cdot \underbrace{\frac{H(I_k)}{\bar{l}}}_{=:R_{Map}}. \tag{3}$$

By applying the chain rule of entropy, the code rate of the intraframe redundancy may be simplified further. Thus, for a first-order Markov source, the code rate R_{corr} for the intraframe redundancy may be expressed as

$$R_{corr} = \frac{H(I_k) + (K-1) \cdot H(I_k|I_{k-1})}{K \cdot H(I_k)} \approx \frac{H(I_k|I_{k-1})}{H(I_k)}.$$

The last approximation holds for a long block length $K \gg 1$.

III. Even-Weight Variable-Length Codes

In the following, we propose a simple VLC construction which provides good compression properties and at the same time guarantees a minimum Hamming distance of $d_{min} = 2$ between code sequences of equal length. These properties are especially useful for the design of efficient encoding schemes for iterative source-channel decoding, which will be discussed in Section IV.

In order to satisfy the distance constraint $d_{min} = 2$, we only consider codewords with even Hamming weight in the codeword set $\mathcal{VLC}$ of the VLC; further constraints as symmetry or reversibility are neglected. Accordingly, we refer to the resulting VLC as even-weight variable-length code (EW VLC). It can be seen as a simple variable-length error-correcting code [5].

The construction of the EW VLC for a set $\mathcal{I}$ of source symbols I_k is parametrized by the minimum code word length l_{min}. In the following, l_{min} is set to the minimum word length of the Huffman code, derived for the underlying source distribution $\Pr(I_k)$. The derivation of the codeword set $\mathcal{VLC}$ for the EW VLC can then be summarized as follows:

1. Initialization of
   - the current code word length $l = l_{min}$,
   - the number of assigned code words $A = 0$, and
   - the set of available length-l codewords $\underline{\mathcal{V}}_l = \{\mathbf{b} \,|\, \mathbf{b} \in \mathbb{B}^l\}$.
2. The code word candidates $\mathbf{b}$ available in the set $\underline{\mathcal{V}}_l$ are separated into the set of code words with *even* Hamming weight

   $$\underline{\mathcal{E}}_l := \{\mathbf{b} \,|\, \mathbf{b} \in \underline{\mathcal{V}}_l,\ w_H(\mathbf{b}) \text{ is even}\}$$

   and into the set of code words with *odd* Hamming weight

   $$\underline{\mathcal{O}}_l := \{\mathbf{b} \,|\, \mathbf{b} \in \underline{\mathcal{V}}_l,\ w_H(\mathbf{b}) \text{ is odd}\}.$$

3. We assign a number of $\min\{|\underline{\mathcal{E}}_l|, |\mathcal{I}| - A\}$ code words $\mathbf{b} \in \underline{\mathcal{E}}_l$ with even Hamming weight to the code word set $\mathcal{VLC}$ of the EW VLC.
4. The number of assigned code words, the set of available code words, and the current code word length are incremented according to

   $$\begin{aligned} A &= A + \min\{|\underline{\mathcal{E}}_l|, |\mathcal{I}| - A\} \\ \underline{\mathcal{V}}_{l+1} &= \{\mathbf{b} = [b_1, \ldots, b_{l+1}] \,|\, [b_1, \ldots, b_l] \in \underline{\mathcal{O}}_l\} \\ l &= l + 1. \end{aligned}$$

5. If all code words are assigned ($A = |\mathcal{I}|$), the code construction is completed; otherwise return to step 2.

After constructing the code word set $\mathcal{VLC}$, the codewords are assigned to the symbols I_k in $\mathcal{I}$ such that highly probable symbols are represented by short codewords.

Even though the distribution of the source symbols I_k is not considered for the code construction, Table I verifies the good compression properties of the EW VLC. For the distribution of the English alphabet and for a Laplacian, a Gaussian, and a uniform distribution with $|\mathcal{I}| = 32$, it compares the code rate R_{Map} of the EW VLC to the code

rates achieved by the Huffman code and the asymmetric and symmetric reversible variable-length codes (RVLCs) from [3], [4]. It becomes obvious that the EW VLC outperforms the RVLCs with respect to their compression properties. Furthermore, for a Laplacian and a Gaussian distribution, the performance of the EW VLC is close to that of the Huffman code.

	Code rate R_{Map}			
	Engl. alphabet	Laplace	Gaussian	uniform
Huffman	0.9916	0.9926	0.9899	1
EW-VLC	0.9726	0.9818	0.9736	0.9091
asym. RVLC [3]	0.9612	0.9638	0.9568	1
sym. RVLC [3]	0.8640	0.9122	0.8944	0.7692
asym. RVLC [4]	0.9466	0.9657	0.9484	0.9091
sym. RVLC [4]	0.8307	0.8993	0.8852	0.7143

TABLE I

COMPARISON OF THE CODE RATE R_{Map} FOR THE EVEN-WEIGHT VARIABLE-LENGTH CODE (EW VLC) ($d_{min} = 2$), THE HUFFMAN CODE ($d_{min} = 1$), AND THE REVERSIBLE VARIABLE-LENGTH CODES (RVLCS) PROPOSED IN [3] ($d_{min} = 1$) AND [4] ($d_{min} = 2$).

IV. ENCODER DESIGN FOR ITERATIVE SOURCE-CHANNEL DECODING AND EQUALIZATION

We now address the optimization of the source and channel encoder in Fig. 1 for iterative source-channel decoding. The properties of established bit mappings and variable-length codes with respect to the design guidelines for serial concatenated channel codes will be analyzed. We will show in the following that both conventional bit mappings and VLCs lead to several drawbacks, which can be avoided by employing EW VLCs proposed in the previous section. For both EW VLCs and a scheme with fixed-length source encoding by employing the optimized bit mappings from [39], we finally present the results of an optimization of the inner channel encoder and precoder for the AWGN channel and the ISI channel, respectively.

A. Analysis of Serial Concatenated Interleaved Codes and Design Rules

Generally, the optimization of concatenated encoders in conjunction with iterative decoding can be approached from two different points of view: on the one hand, the component codes have to be chosen in such a way that good codes with respect to the distance properties are generated. On the other hand, we have to ensure in the code design that convergence of the iterative decoder can be achieved. Both aspects are important for the reliability of the resulting transmission system: a system suffering from a high error floor is as much useless as a strong code that can not be decoded.

1) Distance Properties: An upper bound on the bit error probability P_{err} for serial concatenated channel codes was derived in [36]. The analysis of the upper bound leads to important insights into the design of powerful serial concatenated codes. It shows that serial concatenated codes – if properly designed – can benefit from an interleaver gain. It is defined as the factor by which the P_{err} is decreased for an increasing interleaver length N. Generally, an interleaver gain can be obtained [36]

1) if the minimum Hamming distance $d_{min}^{(o)}$ of the outer code satisfies $d_{min}^{(o)} \geq 2$ and
2) if the inner encoder is recursive.

If these conditions are satisfied, the interleaver gain is given by [36]

$$P_{err} \propto N^{-\lceil \frac{d_{min}^{(o)}}{2} \rceil}.$$

Obviously, a large minimum Hamming distance $d_{min}^{(o)}$ of the outer encoder leads to a large interleaver gain. Furthermore, it is beneficial to maximize the effective free distance of the inner code and to choose the outer encoder as non-recursive [36].

2) Convergence Analysis: A powerful framework for the analysis of the convergence behavior of the iterative decoder is given by extrinsic information transfer characteristics (EXIT charts) [38]. Based on information theoretic measures, it allows for precise predictions of the performance of serial concatenated codes under iterative decoding, without running the iterative decoder.

For an EXIT charts analysis, SISO decoders are treated as information filters. They are characterized by the amount of mutual information between their extrinsic output and the corresponding quantity at the encoder, given the mutual information between the *a priori* input and the underlying symbols at the encoder.

In the following, we refer to the mutual information at the *a priori* input of the source decoder and the channel decoder / equalizer as

$$\mathrm{I}_{apri}^{(s)} := \mathrm{I}(A_n^{(s)}; B_n) \quad \text{and} \quad \mathrm{I}_{apri}^{(c)} := \mathrm{I}(A_{n'}^{(c)}; B'_{n'}),$$

respectively, and to the mutual information at the extrinsic output of the source decoder and the channel decoder / equalizer as

$$\mathrm{I}_{extr}^{(s)} := \mathrm{I}(E_n^{(s)}; B_n) \quad \text{and} \quad \mathrm{I}_{extr}^{(c)} := \mathrm{I}(E_{n'}^{(c)}; B'_{n'}),$$

respectively. Furthermore, we denote the mutual information $\mathrm{I}(Y_m; X_m)$ between the symbols Y_m and X_m at the output and input of the communication channel as $\mathrm{I}_c := \mathrm{I}(Y_m; X_m)$. Correspondingly, the EXIT characteristics specifying the source decoder and the channel decoder / equalizer are given by the mappings

$$\begin{aligned} \mathcal{X}^{(s)} :\ \mathrm{I}_{apri}^{(s)} &\mapsto \mathrm{I}_{extr}^{(s)} = \mathcal{X}^{(s)}(\,\mathrm{I}_{apri}^{(s)}\,) \qquad \text{and} \\ \mathcal{X}^{(c)} :\ \mathrm{I}_{apri}^{(c)} &\mapsto \mathrm{I}_{extr}^{(c)} = \mathcal{X}^{(c)}(\,\mathrm{I}_{apri}^{(s)}\,|\,\mathrm{I}_c\,). \end{aligned}$$

Note that, since the inner decoder also utilizes the *a priori* input for the channel observations, the EXIT characteristic of the inner channel decoder / equalizer is conditioned on I_c. Generally, EXIT characteristics represent bijective monotonically increasing functions from the interval $[0, 1]$ to $[0, 1]$, and thus, the inverse mappings ${\mathcal{X}^{(s)}}^{-1}$ and ${\mathcal{X}^{(c)}}^{-1}$ are well defined.

In order to analyze the convergence behavior of the iterative decoder, the EXIT characteristic $\mathcal{X}^{(c)}$ of the inner (channel) decoder and the inverse EXIT characteristic ${\mathcal{X}^{(s)}}^{-1}$ of

the outer (source) decoder are plotted into the same diagram. The inverse has to be applied for the outer encoder since the extrinsic output of the one decoder becomes the *a priori* input of the other decoder. Predictions of the convergence behavior can be obtained by drawing a decoding trajectory (cf. [38]) between the two characteristics. Convergence is possible if the inner EXIT characteristic $\mathcal{X}^{(c)}$ lies above $\mathcal{X}^{(s)^{-1}}$.

An intersection of the EXIT characteristics specifies the fixpoint of the iterative decoding procedure. Correspondingly, in order to avoid a convergence towards high bit error rates, the components of the encoder should be chosen in such a way that the EXIT charts intersect at $(I_{apri}, I_{extr}) = (1,1)$ bit / channel use. As a consequence, the inner encoder must be recursive [37], [38] and the minimum Hamming distance $d_{min}^{(o)}$ of the outer encoder must satisfy $d_{min}^{(o)} \geq 2$.[3] Both recommendations confirm the design guidelines derived from the analysis of the upper bound of the bit error probability in [36].

Another design criterion follows from the area property of the EXIT charts, proved in [43] for the binary erasure channel. It states that the area $\mathcal{A}(\mathcal{X}^{(s)^{-1}})$ under the inverse EXIT characteristic of the outer decoder corresponds to its code rate $R^{(o)}$, while the area $\mathcal{A}(\mathcal{X}^{(c)})$ under the inner EXIT characteristic $\mathcal{X}^{(c)}$ is lower or equal to the ratio of the mutual information I_c of the communication channel and the inner code rate $R^{(i)}$:

$$\mathcal{A}(\mathcal{X}^{(s)^{-1}}) = R^{(o)} \quad \text{and} \quad \mathcal{A}(\mathcal{X}^{(c)}) \leq I_c / R^{(i)}.$$

Since equality holds for $R^{(i)} = 1$, it is thus reasonable to choose inner rate-1 codes. Otherwise, the transmission system may suffer from a capacity loss [43], which may increase the decoding threshold towards higher channel signal-to-noise ratios (SNR).

B. Inverse EXIT Characteristics for the Inner Source Decoder

For both standard and optimized bit mappings and the EW VLC introduced in Section III the inverse EXIT characteristics for the inner source decoder [33] are depicted in Fig. 2. The EXIT characteristics are obtained for source vectors of $K = 20000$ symbols, a correlation coefficient $a = 0.9$, and a 4-bit scalar quantization with the Lloyd-Max quantizer.

As shown in Fig. 2, for standard bit mappings as the Gray mapping or the natural binary mapping, the outer source decoder provides only a low amount of information at its extrinsic output, given perfect *a priori* information ($I_{apri}^{(s)} = 1$ bit / channel use). Early intersections with the EXIT function of the inner decoder are the consequence, leading to a poor performance of the transmission system.

To overcome this problem, optimized mappings have been proposed in [44], [39], which are based on a maximization of the distortion for the case of one-bit errors and on a maximization of the extrinsic information for optimal *a priori* information, respectively. The inverse EXIT characteristic for the mapping from [39] is included in Fig. 2, verifying the superiority of the optimized mappings to the conventional ones. However, we are still not able to obtain iterative decoder convergence at $(I_{apri}, I_{extr}) = (1,1)$ bit / channel use in the EXIT chart.

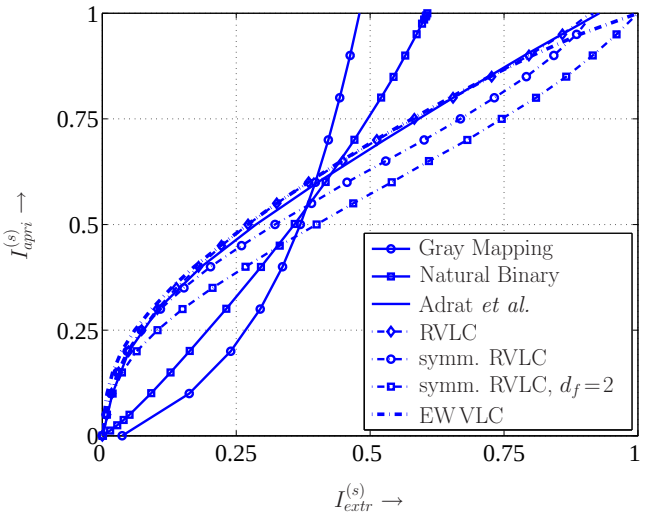

Fig. 2. Inverse EXIT characteristics $\mathcal{X}^{(s)^{-1}}$ of the (outer) source encoder / decoder pair: comparison between standard and optimized bit mappings, reversible VLCs, and the EW VLC for a first-order autoregressive process with correlation coefficient $a = 0.9$, quantized by a 4-bit Lloyd-Max quantizer.

A similar behavior of the iterative decoder can be expected for the asymmetrical RVLC proposed in [3]. By considering an additional symmetry constraint in the RVLC design [3], the robustness can be further improved, however, at the cost of a decreased code rate R_{Map}. In this case, the mean word length $\bar{l}$ is larger than the quantization word length W, i.e., the symmetrical RVLC introduces some redundancy.

Neither the analyzed mappings nor the RVLCs from [3] fulfill the condition $d_{min}^{(o)} \geq 2$. As a consequence, transmission systems which employ one of these codes can generally not benefit from an interleaver gain. RVLCs which satisfy the distance constraint $d_{min}^{(o)} \geq 2$ are proposed in [4]. The inverse EXIT characteristic for the symmetrical RVLC from [4] is included in Fig. 2. Assuming an appropriate (recursive) inner encoder, convergence at $(I_{apri}, I_{extr}) = (1,1)$ bit / channel use becomes possible, and the interleaver gain can be exploited. Unfortunately, as we can see in Table I and conclude from the area under the inverse EXIT characteristic, the code rate is further decreased, i.e., additional redundancy is introduced due to the distance constraint.

This drawback can be avoided with the EW VLC from Section III. As Fig. 2 shows, $(I_{apri}, I_{extr}) = (1,1)$ bit / channel use is achieved in the EXIT chart whereas a slight compression can be obtained compared to the bit mappings with constant word length. Thus, the EW VLC allows for a good convergence behavior of the iterative decoder while maintaining good compression properties at the same time.

[3] Even though this condition is satisfied for channel codes, it will become important for the design of the source encoder in the next section.

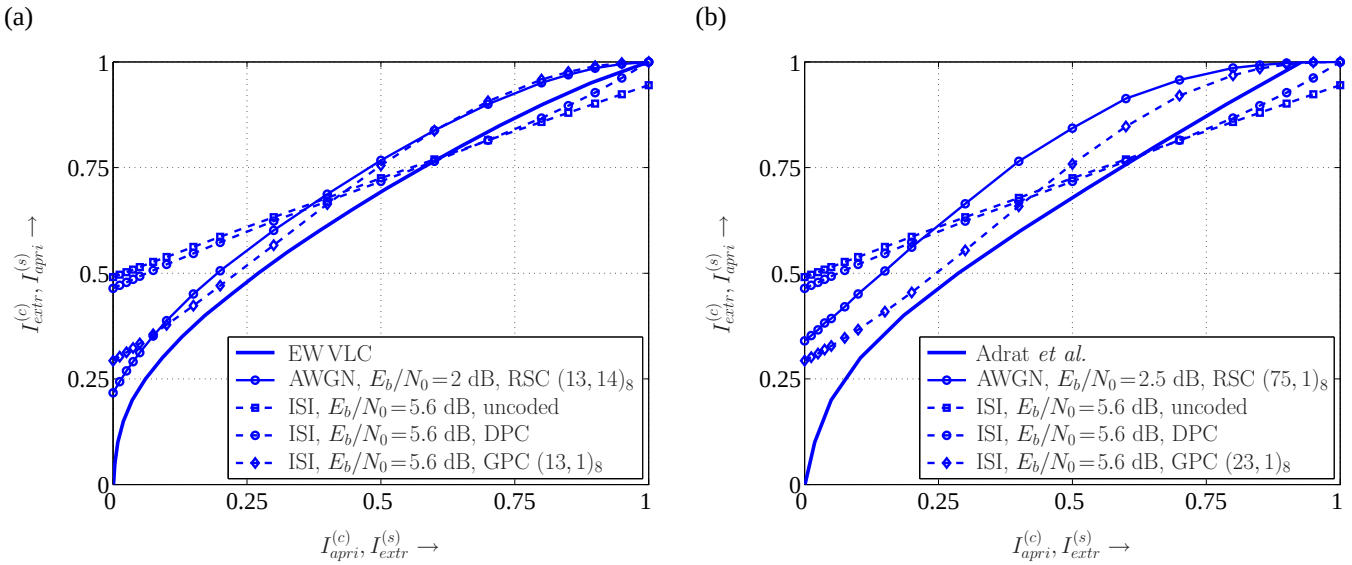

Fig. 3. Optimization of the inner channel encoder / precoder for the EW VLC (a) and the optimized bit mapping from [39] (b): AWGN channel without ISI, uncoded AWGN channel with ISI channel, and precoded AWGN channel with ISI.

C. Code Matching for the Inner and Outer Encoder

In the following, we focus on the design of the inner RSC code / precoder. The goal is to find a good-matching inner code whose EXIT characteristic lies above the inverse EXIT characteristic of the outer source decoder. Therefore, we restrict ourselves to the EW VLC, introduced in the previous section, since it offers the best trade-off between compression capabilities and distance properties. As a benchmarking scheme for our EW VLC-based approach we consider fixed-length quantizer indices with an optimized bit mapping [39] in the source encoding stage.

As Fig. 2 shows, the outer source decoder provides only a small amount of extrinsic information $\mathrm{I}_{extr}^{(s)}$ for $\mathrm{I}_{apri}^{(s)} \leq 0.25\,\mathrm{bit/channel\ use}$ for both EW VLC and optimized bit mapping. Therefore, in order to avoid an early intersection of the EXIT characteristics, the inner channel encoder / precoder has to be chosen such that in absence of *a priori* knowledge ($\mathrm{I}_{apri}^{(c)} = 0\,\mathrm{bit/channel\ use}$) a minimum amount of extrinsic information $\mathrm{I}_{extr}^{(c)}(0) \geq 0.1\,\mathrm{bit/channel\ use}$ is guaranteed.

1) AWGN Channel without ISI: For rate-1 RSC codes, which are obtained by puncturing the systematic bits, it was observed in [38] that only codes whose feedforward polynomials consist of a single coefficient are able to generate extrinsic information $\mathrm{I}_{extr}^{(c)}(0) > 0\,\mathrm{bit/channel\ use}$ without additional *a priori* knowledge. However, especially for a short code memory, these codes have the drawback that only few candidates are available such that the code design becomes quite constrained. In [38], this weakness was compensated by systematic doping, i.e., for RSC codes whose feed-forward polynomials consist of more than one coefficient, a low number of systematic bits was transmitted in addition to the parity bits.

However, this approach poses a problem in our source-channel encoding setup. In order to achieve $\mathrm{I}_{extr}^{(c)}(0) \geq 0.1\,\mathrm{bit/channel\ use}$ the number of additionally transmitted systematic bits would become too large such that the decrease of the coderate R_{RSC} cannot be neglected. As a remedy, in [33] we have applied punctured RSC codes where both systematic and parity bits are pruned from the bit stream in order to find a good-matching rate-1 RSC code. However, due to the high degree of freedom, an optimization becomes fairly complex.

The design of appropriate puncturing patterns can be simplified by considering randomly punctured RSC codes as introduced in Section II-B. The result of the optimization for the EW VLC from Section III is shown in Fig. 3(a). A good-matching code is found by randomly puncturing a fraction $p_{sys} = 92\%$ of the systematic bits and a fraction of $p_{par} = 8\%$ of the parity bits from the memory-3 RSC code with generator polynomials $(13, 14)_8$.

Finally, for the optimized bit mapping from [39] we apply the memory-5 RSC code [45], where the corresponding EXIT characteristic is shown in Fig. 3(b). It is obtained by puncturing all systematic bits from the rate-1/2 mother code with the generator polynomials $(75, 1)_8$. Since in this case the EXIT characteristic for the source decoder does not reach $(I_{apri}, I_{extr}) = (1, 1)\,\mathrm{bit/channel\ use}$ in the EXIT chart, an RSC code with larger memory must be applied.

2) AWGN Channel with ISI: For the analysis of the inner equalizer EXIT characteristic, we employ the memory-4 ISI channel from [46] given by the impulse response

$$h_0(m) = 0.227{\cdot}\gamma_0(m){+}0.46{\cdot}\gamma_0(m{-}1){+}0.6888{\cdot}\gamma_0(m{-}2) + 0.46 \cdot \gamma_0(m-3) + 0.227 \cdot \gamma_0(m-4).$$

It introduces severe ISI to the transmitted data and is thus well suited as test channel for turbo equalization [47]. In the following, we assume perfect knowledge of the channel coefficients $h_0(m)$ at the receiver.

Without additional precoding, the ISI channel can be interpreted as a non-recursive non-binary inner encoder, leading to a violation of the design rules, summarized in

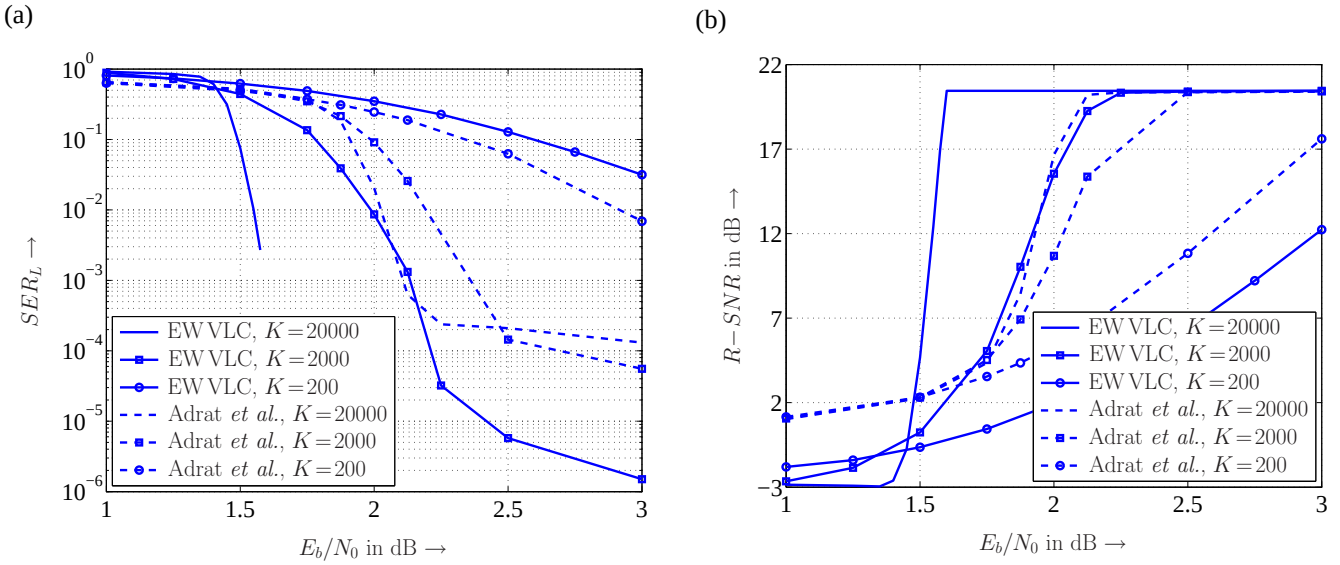

Fig. 4. Comparison between optimized mappings [39] and EW VLCs for the AWGN channel with iterative source-channel decoding: symbol error rate (SER) versus E_b/N_0 (a) and signal-to-noise ration (SNR) versus E_b/N_0 after source reconstruction (b), for varying block lengths $K \in \{200, 2000, 20000\}$.

Section IV-A. Accordingly, we can observe in Fig. 3 that the EXIT characteristic for the APP equalizer applied to the uncoded channel does *not* reach $I_{extr}^{(c)} = 1\,\text{bit}/\text{channel use}$ for $I_{apri}^{(c)} \rightarrow 1\,\text{bit}/\text{channel use}$. Early intersections with the outer source decoder characteristics result for both the EW VLC in Fig. 3(a) and the optimized bit mappings in Fig. 3(b).

A simple approach to make the ISI channel recursive is to apply a differential precoder (DPC) in form of a memory-1 accumulator. However, even though the EXIT characteristic for the equalizer and the differential precoded ISI channel approaches $(I_{apri}, I_{extr}) = (1, 1)\,\text{bit}/\text{channel use}$ in the EXIT chart, early intersections still remain.

To overcome this problem, we consider a generalized precoder (GPC). As described in Section II-B, it is realized by a rate-1 RSC code with feedforward polynomial $G_f = 1$ which is obtained by puncturing all systematic bits from the bit stream. The results of a code search are included in Fig. 3: for the EW VLC (a), the memory-3 RSC code $(13, 1)_8$ offers good properties, allowing for a robust convergence behavior of the iterative decoder / equalizer. As already observed in the AWGN case, the code search for the optimized bit mapping leads to a code with higher memory. We found the memory-4 RSC code $(23, 1)_8$ as a well-suited candidate. The corresponding EXIT characteristic is shown in Fig. 3(b). Note that, since the memory of all considered precoders is lower or equal to the memory of the ISI channel, the decoder complexity stays the same as for the equalization of the uncoded channel.

V. Simulation Results

In the following, we verify the good performance of the even-weight variable-length code (EW VLC) from Section III in the context of iterative source-channel decoding. Monte Carlo simulations are performed for both the BPSK-modulated AWGN channel with and without ISI by using the code constructions from Section IV-C.

The results are presented in Figs. 4 and 5 for the symbol error rate (SER_L) based on the Levenshtein metric[4] and for the distortion in terms of reconstruction signal-to-noise ratio ($R-SNR$). In order to allow a fair comparison between different approaches the channels are parametrized by the channel SNR E_b/N_0 related to the transmit energy per information bit $E_b = E_s/R$. The simulations are carried out for source vectors of $K = 20000$ symbols, a correlation coefficient $a = 0.9$, and a 4-bit scalar quantization with the Lloyd-Max quantizer. For both the EW VLC and the optimized mapping we achieve approximately the same overall code rate of $R \approx 0.66$. All interleavers are realized by s-random interleavers.

A. AWGN Channel without ISI

Fig. 4 shows the good performance of the EW VLC combined with the randomly punctured RSC code $(13, 14)_8$. For a block length of $K = 20000$ symbols and $E_b/N_0 \geq 1.6$ dB, an error-free transmission is achieved after 40 iterations, within 0.6 dB of the capacity limit for $R = 0.66$. Compared to the fixed-length approach with an optimized mapping from [39] and a memory-5 RSC code, a gain of 0.5 dB in channel SNR with respect to clear channel quality can be observed in Fig. 4(b). For the optimized mapping convergence is obtained after 10 iterations, even though the transmission suffers from a residual SER of approximately $2 \cdot 10^{-4}$.

For an intermediate block length of $K = 2000$ symbols the performances of both systems deteriorate. Despite the VLC approach now also shows an error-floor, it still outperforms the optimized mapping: for $E_b/N_0 \geq 1.75\,\text{dB}$ and $K = 2000$ symbols, the achieved distortion is comparable to the one obtained by the fixed-length-based scheme for a block length

[4]The Levenshtein metric of two sequences gives the number of insertions, deletions, and / or substitutions which are needed to transform one sequence into the other. An efficient approximation is proposed in [5].

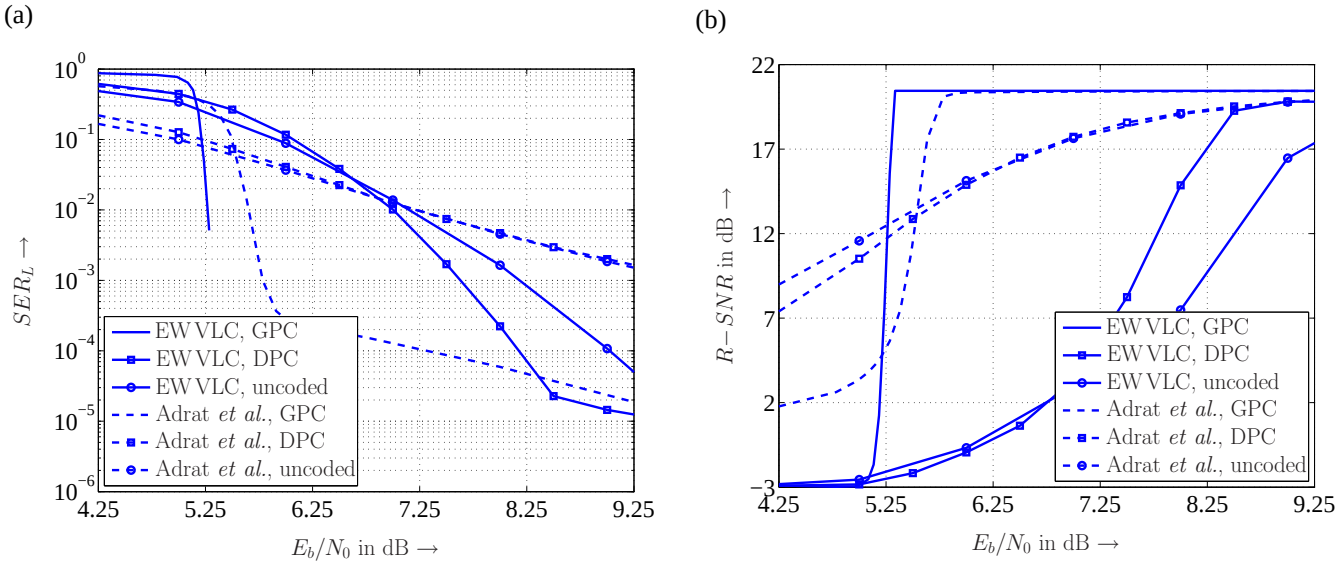

Fig. 5. Comparison between optimized mappings and EW VLCs for the ISI channel (uncoded, differential precoding (DPC), and generalized precoding (GPC)) and iterative source-channel decoding and equalization: symbol error rate (SER) versus E_b/N_0 (a) and signal-to-noise ration (SNR) versus E_b/N_0 after source reconstruction (b).

of $K = 20000$ symbols. If the block length is further reduced to $K = 200$ symbols, the optimized mapping becomes superior for the channel SNR regime shown in Fig. 4.

The SER comparison in Fig. 4(a) for different block / interleaver lengths shows the behavior we expect according to the discussion from Section IV-B: due to a minimum distance of $d_{min}^{(o)} = 1$, the system based on the optimized mapping suffers from a residual error floor for $E_b/N_0 \geq 2.25\,\text{dB}$. In contrast, the EW VLC with $d_{min}^{(o)} = 2$ takes advantage of the available interleaver gain: while the SER only slowly decreases for $E_b/N_0 \geq 2.5\,\text{dB}$ and a block length of $K = 2000$ symbols, no error event could be observed for $E_b/N_0 \geq 1.6\,\text{dB}$ and $K = 20000$ symbols.

B. AWGN Channel with ISI

The results for uncoded and precoded transmission in the presence of ISI are shown in Fig. 5 for a blocklength of $K = 20000$ symbols. The results confirm the poor performance of iterative source decoding and equalization for the uncoded and differentially precoded (DPC) ISI channel, predicted in Section IV-C. For both the EW VLC-based and the mapping-based scheme early intersections between the EXIT characteristics lead to high symbol error rates and high distortions. Compared to the EW VLC, which suffers from synchronization losses, the optimized mapping turns out to be more robust in this environment.

However, significant improvements can be obtained by considering the generalized precoders (GPC) proposed in Section IV-C. For the EW VLC an error-free transmission is now achieved for $E_b/N_0 \geq 5.3$ dB after 50 iterations between the SISO source decoder and the equalizer. In accordance to the results for the AWGN channel without ISI we again observe a gain of 0.5 dB for the EW VLC-based technique compared to the approach based on an optimized mapping, which now shows a slightly decreasing error floor for $E_s/N_0 \geq 6.0\,\text{dB}$.

VI. Conclusions

We have presented a simple variable-length code construction which is well suited for transmission systems employing iterative source-channel decoding. While providing good compression properties compared to, e.g., RVLCs the proposed even-weight variable-length code (EW VLC) guarantees a minimum Hamming distance of two between equal-length code sequences. Both features are the key to transmission systems which are extremely efficient in terms of required overhead for error protection and robust at the same time. As the simulation results for correlated Gauss-Markov sources show, the proposed EW VLC facilitates reliable communication close to the AWGN channel capacity solely by exploiting residual source redundancy. This also holds true if the channel is additionally affected by ISI. Finally, a comparison shows that the proposed EW VLC-based scheme outperforms the best fixed-length bit mapping optimized for iterative source-channel decoding. These results suggest to employ well-designed variable-length codes instead of fixed-length mappings in the context of iterative source-channel decoding.

References

[1] Y. Takishima, M. Wada, and H. Murakami, "Reversible variable length codes," *IEEE Trans. Commun.*, vol. 43, no. 2/3/4, pp. 158–162, Feb./Mar./April 1995.

[2] J. Wen and J. D. Villasenor, "Reversible variable length codes for efficient and robust image and video coding," in *Proc. IEEE Data Compression Conference*, Snowbird, UT, Mar. 1998, pp. 471–480.

[3] C. W. Tsai and J. L. Wu, "On constructing the Huffman-code based reversible variable length codes," *IEEE Trans. Commun.*, vol. 40, no. 9, Sept. 2001.

[4] K. Laković and J. Villasenor, "On design of error-correcting reversible variable length codes," *IEEE Communications Letters*, vol. 6, no. 8, pp. 337–339, Aug. 2002.

[5] V. Buttigieg, *Variable-Length Error-Correcting Codes*, Ph.D. thesis, Department of Electrical Engineering, University of Manchester, Manchester, England, 1995.

[6] V. Buttigieg and P. G. Farrell, "A maximum a-posteriori (MAP) decoding algorithm for variable-length error-correcting codes," in *Codes and Cyphers: Cryptography and Coding IV*, pp. 103–119. The Institute of Mathematics and Its Applications, Essex, England, 1995.

[7] V. B. Balakirsky, "Joint source-channel coding with variable length codes," in *Proc. IEEE Int. Sympos. Information Theory*, Ulm, Germany, June 1997, p. 419.

[8] L. R. Bahl, J. Cocke, F. Jelinek, and J. Raviv, "Optimal decoding of linear codes for minimizing symbol error rate," *IEEE Trans. Inf. Theory*, pp. 294–287, Mar. 1974.

[9] A. H. Murad and T. E. Fuja, "Robust transmission of variable-length encoded sources," in *Wireless Communications and Networking Conference (WCNC)*, New Orleans, LA, Sept. 1999, vol. 2, pp. 968–972.

[10] M. Park and D. J. Miller, "Joint source-channel decoding for variable-length encoded data by exact and approximate MAP sequence estimation," *IEEE Trans. Commun.*, vol. 48, no. 1, pp. 1–6, Jan. 2000.

[11] K. Sayood, H. H. Otu, and N. Demir, "Joint source/channel coding for variable length codes," *IEEE Trans. Commun.*, vol. 48, no. 5, pp. 787–794, May 2000.

[12] K. P. Subbalakshmi and J. Vaisey, "On the joint source-channel decoding of variable-length encoded sources: The BSC case," *IEEE Trans. Commun.*, vol. 49, no. 12, pp. 2052 – 2055, Dec. 2001.

[13] C. Lamy and O. Pothier, "Reduced complexity maximum a posteriori decoding of variable-length codes," in *Proc. IEEE Global Telecommunications Conference*, San Antonio, TX, Nov. 2001, vol. 2, pp. 1410–1413.

[14] J. Wen and J. D. Villasenor, "Soft-input soft-output decoding of variable length codes," *IEEE Trans. Commun.*, vol. 50, no. 5, pp. 689 – 692, May 2002.

[15] M. Bystrom, S. Kaiser, and A. Kopansky, "Soft source decoding with applications," *IEEE Trans. on Circuits and Systems for Video Technology*, vol. 11, no. 10, pp. 1108–1120, Oct. 2001.

[16] L. Perros-Meilhac and C. Lamy, "Huffman tree based metric derivation for a low-complexity sequential soft VLC decoding," in *Proc. IEEE Int. Conf. on Communications*, New York City, NY, May 2002, vol. 2, pp. 783–787.

[17] F. I. Alajaji, N. C. Phamdo, and T. E. Fuja, "Channel codes that exploit the residual redundancy in CELP-encoded speech," *IEEE Trans. on Speech and Audio Processing*, vol. 4, no. 5, pp. 325–336, Sept. 1996.

[18] T. Fazel and T. Fuja, "Robust transmission of MELP-compressed speech: An illustrative example of joint source-channel decoding," *IEEE Trans. Commun.*, vol. 51, no. 6, pp. 973–982, June 2003.

[19] R. Perkert, M. Kaindl, and T. Hindelang, "Iterative source and channel decoding for GSM," in *Proc. IEEE Int. Conf. Acoust., Speech, Signal Processing*, Salt Lake City, UT, May 2001, pp. 2649–2652.

[20] T. Fingscheidt and P. Vary, "Softbit speech decoding: A new approach to error concealment," *IEEE Trans. on Speech and Audio Processing*, vol. 9, no. 3, pp. 240–251, Mar. 2001.

[21] S. M. Heinen, "An optimal MMSE estimator for source codec parameters using intra-frame and inter-frame correlation," in *Proc. IEEE Int. Symp. on Information Theory*, Washington, DC, June 2001, p. 237.

[22] K. Laković, J. Villasenor, and R. Wesel, "Robust joint Huffman and convolutional decoding," in *Proc. IEEE Vehicular Technology Conference (VTC)*, Amsterdam, Netherlands, Sept. 1999, pp. 2551–2555.

[23] K. Laković and J. Villasenor, "Combining variable length codes and turbo codes," in *Proc. IEEE 55th Vehicular Technology Conference Spring*, Birmingham, AL, May 2002, vol. 4, pp. 1719–1723.

[24] M. Jeanne, J.-C. Carlach, and P. Siohan, "Joint source-channel decoding of variable-length codes for convolutional codes and turbo codes," *IEEE Trans. Commun.*, vol. 53, no. 1, pp. 10–15, Jan. 2005.

[25] R. Bauer and J. Hagenauer, "Symbol-by-symbol MAP decoding of variable length codes," in *Proc. 3. ITG Conf. on Source and Channel Coding*, Munich, Germany, Jan. 2000, pp. 111–116.

[26] N. Goertz, "On the iterative approximation of optimal joint source-channel decoding," *IEEE Journal on Sel. Areas in Comm.*, vol. 14, no. 9, pp. 1662–1670, Sept. 2001.

[27] R. Bauer and J. Hagenauer, "On variable length codes for iterative source/channel decoding," in *Proc. IEEE Data Compression Conference*, Snowbird, UT, Mar. 2001, pp. 273–282.

[28] A. Guyader, E. Fabre, C. Guillemot, and M. Robert, "Joint source-channel turbo decoding of entropy-coded sources," *IEEE Journal on Sel. Areas in Comm.*, vol. 19, no. 9, pp. 1680–1696, Sept. 2001.

[29] M. Jeanne, J.-C. Carlach, P. Siohan, and L. Guivarch, "Source and joint source-channel decoding of variable length codes," in *Proc. IEEE Int. Conf. on Communications*, New York, NY, Apr. 2002, vol. 2, pp. 768– 772.

[30] R. Thobaben and J. Kliewer, "Robust decoding of variable-length encoded Markov sources using a three-dimensional trellis," *IEEE Communications Letters*, vol. 7, no. 7, pp. 320–322, July 2003.

[31] J. Kliewer and R. Thobaben, "Iterative joint source-channel decoding of variable-length codes using residual source redundancy," *IEEE Trans. Wireless Commun.*, vol. 4, no. 3, pp. 919–929, May 2005.

[32] C. Lamy and L. Perros-Meilhac, "Low complexity iterative decoding of variable-length codes," in *Proc. Picture Coding Symposium (PCS)*, St. Malo, France, Apr. 2003, pp. 275–280.

[33] R. Thobaben and J. Kliewer, "Low complexity iterative joint source-channel decoding for variable-length encoded Markov sources," *IEEE Trans. Commun.*, vol. 53, no. 12, pp. 2054–2064, Dec. 2005.

[34] A. Hedayat and A. Nosratinia, "On joint iterative decoding of variable-length codes and channel codes," in *Proc. Allerton Conf. on Communications, Control, and Computing*, Monticello, IL, Oct. 2002.

[35] A. Hedayat and A. Nosratinia, "Concatenated error-correcting entropy codes and channel codes," in *Proc. IEEE Int. Conf. on Communications*, Anchorage, AK, May 2003, pp. 3090–3094.

[36] S. Benedetto, D. Divsalar, G. Montorsi, and F. Pollara, "Serial concatenation of interleaved codes: Performance analysis, design, and iterative decoding," *IEEE Trans. Inf. Theory*, vol. 44, no. 3, pp. 909–926, May 1998.

[37] J. Kliewer, A. Huebner, and D. J. Costello, Jr., "On the achievable extrinsic information of inner decoders in serial concatenation," in *Proc. IEEE International Symposium on Information Theory*, Seattle, WA, July 2006.

[38] S. ten Brink, "Code characteristic matching for iterative decoding of serially concatenated codes," *Annals of Telecommunications*, vol. 56, no. 7-8, pp. 394–408, July-August 2001.

[39] M. Adrat and P. Vary, "Iterative source-channel decoding: Improved system design using EXIT charts," *EURASIP Journal on Applied Signal Processing*, vol. 2005, no. 6, pp. 928–941, 2005.

[40] J. Hagenauer, E. Offer, and L. Papke, "Iterative decoding of binary block and convolutional codes," *IEEE Trans. Inf. Theory*, vol. 42, no. 2, pp. 429–445, Mar. 1996.

[41] X. M. Chen and P. A. Hoeher, "Blind turbo equalization for wireless DPSK systems," in *Proc. Int. ITG Conf. on Source and Channel Coding*, Berlin, Germany, Jan. 2002, pp. 371–378.

[42] A. V. Oppenheim, R. W. Schafer, and J. R. Buck, *Discrete-Time Signal Processing*, Prentice Hall, New Jersey, 1999.

[43] A. Ashikhmin, G. Kramer, and S. ten Brink, "Extrinsic information transfer functions: Model and erasure channel properties," *IEEE Trans. Inf. Theory*, vol. 50, no. 11, pp. 2657–2673, Nov. 2004.

[44] J. Hagenauer and N. Goertz, "The turbo principle in joint source-channel coding," in *Proc. IEEE Information Theory Workshop (ITW)*, Paris, Fance, Apr. 2003, pp. 275–278.

[45] M. Adrat and P. Vary, "TURBO error concealment of mutually independent source codec parameters," in *Proc. Int. ITG Conf. on Source and Channel Coding*, Erlangen, Germany, Jan. 2004, pp. 287–294.

[46] J. Proakis, *Digital Communications*, John Wiley & Sons, Singapore, 1995.

[47] M. Tüchler, R. Koetter, and A. Singer, "Turbo equalization: Principles and new results," *IEEE Trans. Commun.*, vol. 50, no. 5, pp. 754–767, May 2002.